J. Membrane Biol. 122, 97–110 (1991)
0022263191000858

The Journal of
Membrane Biology

Muscarinic Responses of Gastric Parietal Cells

Jonathan M. Wilkes, Masayoshi Kajimura, David R. Scott, Stephen J. Hersey,† and George Sachs
Center for Ulcer Research and Education, Department of Medicine, University of California at Los Angeles, Los Angeles, California 90073, and †Department of Physiology, Emory University, Atlanta, Georgia 30322

Summary. Isolated rabbit gastric glands were used to study the nature of the muscarinic cholinergic responses of parietal cells. Carbachol (CCh, 100 μM) stimulation of acid secretion, as measured by the accumulation of aminopyrine, was inhibited by the M1 antagonist, pirenzepine, with an IC_{50} of 13 μM; by the M2 antagonist, 11,2-(diethylamino)methyl-1 piperidinyl acetyl-5,11-dihydro-6H-pyrido 2,3-b 1,4 benzodiazepin-6-one (AF-DX 116), with an IC_{50} of 110 μM; and by the M1/M3 antagonist, diphenylacetoxy-4-methylpiperidinemethiodide (4-DAMP), with an IC_{50} of 35 nM. The three antagonists displayed equivalent IC_{50} values for the inhibition of carbachol-stimulated production of $^{14}CO_2$ from radiolabeled glucose, which is a measure of the turnover of the H,K-ATPase, the final step of acid secretion. Intracellular calcium levels were measured in gastric glands loaded with FURA 2. Carbachol was shown to both release calcium from an intracellular pool and to promote calcium entry across the plasma membrane. The calcium entry was inhibitable by 20 μM La^{3+}. The relative potency of the three muscarinic antagonists for inhibition of calcium entry was essentially the same as for inhibition of acid secretion or pump related glucose oxidation. Image analysis of the glands showed the effects of carbachol, and of the antagonists, on intracellular calcium were occurring largely in the parietal cell. The rise in cell calcium due to release of calcium from intracellular stores was inhibited by 4-DAMP with an IC_{50} of 1.7 nM, suggesting that the release pathway was regulated by a low affinity M3 muscarinic receptor or state; Ca entry and acid secretion are regulated by a high affinity M3 muscarinic receptor or state, inhibited by higher 4-DAMP concentrations (>30 nM), suggesting that it is the steady-state elevation of Ca that is related to parietal cell function rather than the $[Ca]_i$ transient. Displacement of ^3H N-methyl scopolamine (NMS) binding to purified parietal cells by CCh showed the presence of two affinities for CCh, but only a single affinity for 4-DAMP and lower affinity for pirenzepine and AFDX 116, providing further evidence for the parietal cell location of the $[Ca]_i$ response. Elevation of steady-state $[Ca]_i$ levels with either ionomycin or arachidonic acid did not replicate M3 stimulation of acid secretion or glucose oxidation, hence elevation of $[Ca]_i$ is necessary but not sufficient for acid secretion.

Key Words acid secretion · carbachol · gastric glands · digital image analysis · intracellular calcium · muscarinic receptor subtype · muscarinic binding · parietal cell

Introduction

Acid secretion by the gastric parietal cell is known to be regulated in part by cholinergic stimulation. Analysis of the mechanisms underlying this stimulation is complicated by the recognition that regulation may be due to a direct action on the parietal cell or to indirect actions such as the release of gastrin (Schubert, Bitar & Makhlouf, 1982) or histamine (Hirschowitz & Molina, 1983). In order to identify further the mechanisms responsible for the direct stimulation of the parietal cell, it is necessary to employ in vitro preparations such as the isolated gastric gland used in the present studies. Moreover, since even in vitro preparations exhibit interactive responses between cholinergic agonists and histamine (Berglindh, 1977*a*; Soll, 1978) and secretagogue-mediated histamine release (Bergquist & Obrink, 1979) care must be taken to isolate the cholinergic response by using histamine H2-receptor antagonists such as cimetidine in the preparation which prevents any consequences of these interactions.

Previous studies with isolated gastric glands and parietal cells (Berglindh, Helander, & Obrink, 1976; Muallem & Sachs, 1985) have shown that direct stimulation by cholinergic agonists leads to a transient increase of acid secretion which peaks at about 20 min and returns to basal levels by about 90 min. This contrasts to the stimulation by histamine, which results in a sustained and larger increase of acid production (Berglindh et al., 1976; Chew et al., 1980). A second difference between histaminergic and cholinergic stimulation lies in the intracellular second messengers which mediate the responses. In the case of histamine, the second messenger has been shown to be mainly cyclic AMP (Chew et al., 1980). Cholinergic stimulation of the parietal cell does not alter cyclic AMP levels, but rather induces a rise of intracellular calcium ($[Ca^{2+}]_i$), (Muallem & Sachs 1985; Chew & Brown 1986; Negulescu, Reenstra & Machen, 1989). Removal of Ca from the medium (Berglindh, Sachs & Takeguchi, 1980) or blockade of Ca entry (Muallem & Sachs, 1985) abolish the cholinergic secretory response of the parietal cell.

These observations have led to the hypothesis that cholinergic stimulation depends on changes of $[Ca^{2+}]_i$. Since cholinergic agonists induce a biphasic response of $[Ca^{2+}]_i$ which is due to release of Ca^{2+} from an intracellular pool and to entry of Ca^{2+} across the plasma membrane (Muallem & Sachs, 1985; Negulescu et al., 1989) and Ca removal from the medium also depletes the intracellular pool by prevention of reloading, it is not clear whether Ca entry, Ca release, or both correlate with the changes in secretory function.

Indeed recent studies of $[Ca^{2+}]_i$ have stated that there is a correlation between acid secretion and the release of calcium from intracellular pools (Negulescu et al., 1989), i.e., the initial peak of $[Ca^{2+}]_i$ although this is in contrast to studies recently reported on peptic cell function (Sutliff et al., 1989). It is also not known whether both phases are mediated by separate receptors or different states of the same receptor, given that there are five different muscarinic receptors (Hulme, Birdsall & Buckley, 1990). The present studies were conducted in order to develop additional information on the relationship between cholinergic stimulation of acid secretion and transient or steady-state changes of $[Ca^{2+}]_i$. This relationship was tested with respect to the action of selective muscarinic antagonists, thus allowing information on the probable subtype of receptor which mediates the responses. The results demonstrate that the two phases of $[Ca^{2+}]_i$ increase may be distinguished on the basis of sensitivity to the antagonist, 4-DAMP or the C kinase activator, TPA. The acid secretory responses were found to correlate with the steady-state increase of $[Ca^{2+}]_i$ due to entry of Ca^{2+} but not with the initial transient peak of $[Ca^{2+}]_i$ due to release of Ca^{2+} from an intracellular pool in contrast to previous interpretations. Comparison of the action of various antagonists showed that the receptor mediating secretory responses of the parietal cell and the changes of $[Ca^{2+}]_i$ was of the M_3 subclass, and that there were two affinities for CCh displacement of ^{3}H-NMS binding to purified parietal cells. The high affinity M3 binding of CCh would correspond to low affinity 4-DAMP binding and results in steady-state elevation of $[Ca^{2+}]_i$. The low affinity binding of CCh would correspond to high affinity 4-DAMP binding and results in Ca^{2+} release. The functional response of the parietal cell therefore stems from Ca entry not Ca release. Alternative means of elevating $[Ca^{2+}]_i$ were unsuccessful in stimulating acid secretion. It appears that steady-state elevation of $[Ca]_i$ is a necessary but not sufficient condition for the secretory response of the parietal cell.

Materials and Methods

Gastric Gland Preparation

Gastric glands were isolated from the gastric mucosa of New Zealand White rabbits as described previously (Berglindh et al., 1976; Chew et al., 1980; Hersey et al., 1981). In brief, the stomach was perfused under pressure with phosphate buffered saline (PBS), removed, and rinsed with PBS. The mucosa was removed by blunt dissection and minced with scissors. The mucosal fragments were resuspended in incubation medium containing in mM: NaCl, 132.4; KCl, 5.4; Na_2HPO_4, 5.0; NaH_2PO_4, 1.0; $MgSO_4$, 1.2; $CaCl_2$, 1.0; and HEPES, 10.0. The initial pH was adjusted to 7.2, and glucose (2 mg/ml) and bovine serum albumin (2 mg/ml) were added. For the digestion, collagenase (type D, Boehringer Mannheim Biochemicals, New York) was added to a final concentration of 15 mg/50 ml, and the mucosal suspension was incubated at 37C° with stirring for 20–35 min under an atmosphere of 95% O_2/5% CO_2. After the incubation period, the glands were filtered through nylon mesh and rinsed by sequential resuspension and sedimentation in incubation medium.

Aminopyrine Accumulation

Formation of an acid gradient by isolated gastric glands was determined from the accumulation of 14C-aminopyrine as described previously (Berglindh et al., 1976; Chew et al., 1980; Hersey et al., 1981). Aliquots of gastric gland suspension (10 mg wet wt/ml) were incubated at 37°C for 20 min in incubation medium containing 0.05 μCi/ml ^{14}C-aminopyrine (90 mCi/mmol; New England Nuclear, Boston, MA). Cimetidine (10^{-4} M) was included in all incubations in order to eliminate any affect of endogenous histamine. The glands were incubated in the presence or absence of carbachol and varying concentrations of the muscarinic antagonists as appropriate. Following the incubation period, the glands were pelleted by centrifugation, the supernatant removed, and the pellet digested with HNO_3. Radioactivity in aliquots of the supernatant and digested pellet was determined by scintillation counting. A correction for aminopyrine accumulation unrelated to acid secretion was obtained from samples incubated in the presence of 20 mM NaSCN (Hersey et al., 1981). The specific accumulation of aminopyrine is expressed as the ratio of aminopyrine concentration in gland water to the concentration in the bathing medium.

$^{14}CO_2$ Production from Glucose

The evolution of CO_2 from glucose was employed as an indirect measure of the activity of the H.K-ATPase, the gastric proton pump (Hersey, 1977; Fryklund et al., 1990). For these experiments, the gastric glands were rinsed and suspended in an incubation medium that contained a reduced concentration of glucose (0.5 mg/ml) and 10^{-4} M cimetidine. 1 ml of medium containing appropriate reagents and 0.5 μCi of D-[U-^{14}C]glucose (270 mCi/mmol) was placed into a Kontes centerwell incubation flask with a sidearm. A 13 × 26 mm piece of Whatman #1 filter paper was placed in the centerwell with 100 μl of 2 N KOH to absorb the evolved CO_2. The incubation was initiated by addition of 1 ml gastric gland suspension (2–5 mg dry wt/ml, final dilution). The

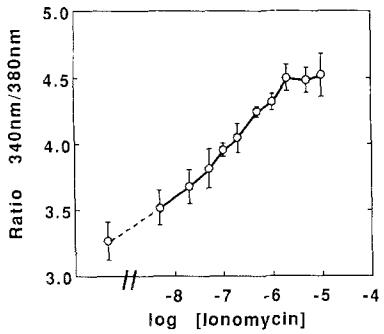

Fig. 1. Titration of calcium loading of gastric glandular cells by ionomycin. Gastric glands, loaded with FURA2 as described in the text, were suspended at 20 mg/ml in monitoring solution. A cumulative dose response to added ionomycin was constructed by allowing the gland suspension to equilibrate for 5 min following each addition then determining the observed ratio between fluorescence at 340 and 380 nm. Data points represent mean + SD for three determinations

incubations were carried out at 37C° for 40 min in a shaking water bath. The incubation was terminated by the addition of 6 N HCl injected through the sidearm of the flask. The flasks were allowed to sit at room temperature for at least 1 hr to assure complete trapping of CO_2. The amount of $^{14}CO_2$ produced was determined by counting the entire contents of the centerwell in a liquid scintillation counter using Hionicfluor (Packard Inst.) as the cocktail.

Monitoring of Intracellular Calcium

Intracellular calcium was monitored as previously described (Muallem & Sachs, 1985) using the fluorescent probe FURA2 (Grykiewicz, Poenie & Tsien, 1985). Gastric glands were loaded with the indicator using the hydrolyzable ester, FURA2-AM, as follows. Glands were resuspended at a concentration of 100 mg wet wt/ml in a monitoring solution containing in mM: NaCl, 100; KCl, 5.4; $MgSO_4$, 1.2; $CaCl_2$, 1.0; HEPES, 20; pyruvate, 10; ascorbate, 10; fumarate, 10; glutamate, 10; and BSA 2 mg/ml. The initial pH was 7.4. FURA2-AM (1 mM in DMSO) was added to a final concentration of 4 μM and the glands were incubated for 35 min at 37°C with gentle agitation. Following the loading period, the glands were rinsed by centrifugation and resuspended in the monitoring solution containing 10^{-4} M cimetidine at a concentration of 10–20 mg/ml.

Measurement of intracellular calcium ($[Ca^{2+}]_i$) in gastric gland suspensions was carried out with a SPEX 1681 dual wavelength spectrofluorimeter, and analyzed with DM3000 cation-measuring software. Gland suspensions were placed in the fluorimeter cuvette and maintained at 37C° with constant stirring. FURA2 fluorescence was monitored using alternating excitation wavelengths of 340 and 380 nm and an emission wavelength of 505 nm.

Entry of calcium into gastric glandular cells, mediated by the calcium ionophore, ionomycin, was titrated by observing the ratio of 340 to 380 nm fluorescence 5 min following the addition of ionomycinin a cumulative dose-response experiment. Maximal ratios, indicating saturating calcium concentrations, were observed at ionomycin concentrations greater than 1 μM (*see* Fig. 1). In subsequent experiments saturating and zero calcium levels were determined following the addition of ionomycin (2–5 μM) and EGTA (20 mM), respectively. These values were not different when digitonin was used to saturate the intracellular dye.

Calcium concentrations were calculated from the ratio of 340 to 380 fluorescence, using a K_d value for FURA2 of 224 nM. In control experiments, autofluorescence associated with gastric glands under the conditions of the experiments was unaffected by the treatments utilized and was less than 15% of the minimum observed ratio signal from FURA2-loaded glands. No subsequent adjustment was made, therefore, for this parameter.

In the absence of secretagogues, the fluorescence ratio monitored from FURA2-loaded glands was constant over the time course of a typical experiment, indicating negligible leakage of dye into the monitoring medium. Leakage into a medium containing 1 mM Ca^{2+} would produce considerable upward drift in this value.

Analysis of Inhibition Data

The concentration dependency of the inhibition of the above cellular responses to 100 μM carbachol by muscarinic antagonists, expressed in terms of percentage inhibition from control, were analyzed by nonlinear regression analysis, utilizing the Enzfit program (Elsevier Biosoft). Values quoted are mean and standard error derived by the program. Standard errors were computed by the matrix inversion method and are useful for indicating the accuracy of the fitted function.

Image Analysis

Intracellular calcium in individual cells was monitored using FURA2 fluorescence measured with an image analysis system. The glands were loaded with FURA2 as described above and placed on a poly-D-lysine coated coverslip which served as the observation port in a perfusion chamber. Monitoring solution, maintained at 37°C, was continuously perfused through the chamber. The glands were observed through a Nikon Fluo 40 objective with a Zeiss Axiomat microscope in the epifluorescence mode using a long pass filter cutoff at 510 nm. Alternating excitation wavelengths of 350 and 380 nm were provided by the SPEX 1681 fluorimeter using a coupled chopper mechanism. The imaged field was monitored by a COHU ISIT camera. Image pairs were captured (less than 1 sec apart) under the control of TARDIS software, and stored as digitized 256 gray level images. Subsequent digital image analysis was performed under the control of TARDIS software using a Joyce-Loebl Magical Image processor. Following subtraction of background fields, R_{max} and R_{min} were determined from image pairs of glands equilibrated with ionomycin and EGTA. These parameters were used by the image processor to relate the ratio of each 350 nm, 380 nm pixel pair to calcium concentration, using a K_d value of 224 nM. Images were processed in pairwise fashion, with a threshold gray level of 8. The mean calibrated calcium level over successive frames for individual cells in the field was measured over a user-defined area.

Binding Studies

Cell Separation

Parietal cells were purified by an adaptation of previously established methods (Muallem et al., 1985). They were purified by step gradient centrifugation on a Nycodenz gradient. Gastric glands

Table 1. Response of isolated gastric glands to 100 μM carbachol

Response assayed	Units	Control values	Stimulated values
[^{14}C]-aminopyrine accumulation	None	25 ± 3 (6)	88 ± 6 (6)[a]
$^{14}CO_2$ evolution	nmol CO_2/hr/mg	102.9 ± 11.6 (21)	172.5 ± 14.8 (12)[a]
Steady-state elevated $[Ca^{2+}]_i$	nmol/liter	267 ± 85 (38)	671 ± 157 (7)[a]
Peak transient $[Ca^{2+}]_i$	nmol/liter	267 ± 85 (38)	1623 ± 409 (7)[a]

Rabbit gastric glands, isolated as described in the text, were assayed for the response of various cellular properties to 100 μM carbachol. The responses of the glands are expressed as mean ± SD for (n) determinations.
[a] $P < 0.05$ by Students t test.

isolated as above were resuspended in incubation medium as above and further digested with pronase (0.3 mg/ml, Calbiochem) at 37C° for 20–30 min. The cell suspension was rinsed twice by low speed centrifugation (300 × g for 5 min) in the presence of 100 μM cimetidine, to correspond with the functional studies. The final cell pellet was resuspended into 20 ml of 5.5% wt/vol Nycodenz solution and 10 ml of this suspension was layered on top of 12 ml of a 13.8% wt/vol Nycodenz solution in a 50 ml Falcon plastic centrifuge tube and centrifuged for 10 min at 800 × g (Muallem et al., 1985). The average purity of parietal cells at the interface was 77 ± 4.3% (SEM), $n = 6$, and these were washed twice with incubation medium (Muallem et al., 1985, 1988).

NMS Binding and Displacement

Between 2 and 4 × 10^6 cells were transferred to 1.5 ml conical centrifuge tubes in 1 ml of medium and incubated in the presence and absence of muscarinic ligands. ^{3}H-N methyl scopolamine (NMS, 78.9 Ci/mmol) was used at a concentration of 0.9 nM for displacement experiments and over a range of 30 to 3000 pM for saturation estimates. After 45 min incubation at 37C°, the cell suspension was chilled on ice and centrifuged for 1 min at 0C° and 10,000 × g. The supernatant was aspirated and the cell pellet washed once with 1.3 ml phosphate buffered saline. After drying overnight, the pellet was dissolved in 100 μl 1 N NaOH, dissolved in scintillation cocktail and counted in a liquid scintillation counter. Specific binding was defined as the difference in binding in the absence and presence of 10 μM atropine.

Data Analysis

The NMS binding values were fitted by means of a nonlinear regression analysis (Pfit, Elsevier Biosoft) and analyzed as previously described (Kajimura et al., 1990).

The binding fitted the equation

$$Y = B_{max} \cdot L/(K_d + L)$$

where Y is the specific binding of NMS at a concentration of L and B_{max} is the total binding and K_d is the dissociation constant of NMS, respectively.

Displacement of ^{3}H-NMS by CCh or 4-DAMP was analyzed by either a 1- or a 2-site model equation as follows

$$Y = 100 \cdot IC_{50}/(IC_{50} + L) \quad (2)$$

or

$$Y = A \cdot IC_{50H}/(IC_{50H} + L) + (100 - A) \cdot IC_{50L}/(IC_{50L} + L) \quad (3)$$

where Y is the specific binding at concentration L of ligand, IC_{50H} and IC_{50L} are the IC_{50} values for the high and low affinity sites or states. The dissociation constants of the muscarinic ligands were calculated from the equation (Cheng & Prusoff, 1973)

$$K_d = IC_{50}/(1 + [^3\text{H-NMS}]/K_d^*)$$

where K_d is the dissociation constant of the ligand, K_d^* is the dissociation constant for NMS in the parietal cell, and [^{3}H-NMS] is concentration used for the displacement experiments. The slope, n, of the displacement curve was calculated by a linear regression analysis using the equation

$$\text{Log}([RL_o^*]/[RL_i^*] - 1) = n(\log[L_i] - \log IC_{50}) \quad (5)$$

where $[L_i]$, $[RL_o^*]$ and $[RL_i]$ are the concentration of the ligand and the amount of NMS binding in the presence and absence of ligand, respectively.

Chemicals

All of the chemicals used were of the highest purity available. The sources for some of the reagents were as follows: FURA2-AM was from Molecular Probes (Eugene, OR), collagenase (Type D) was from Boehringer Mannheim Biochemicals (Indianapolis, IN), 4-DAMP and AF-DX 116 were generous gifts from Allergan (Irvine, CA).

Results

Intracellular Calcium

Monitoring of the $[Ca^{2+}]_i$ in gastric glands, using the fluorescent probe FURA2, demonstrated dramatic increases upon additon of carbachol, thus confirming previous observations (Muallem & Sachs, 1985; Chew & Brown 1986; Negulescu et al., 1989).

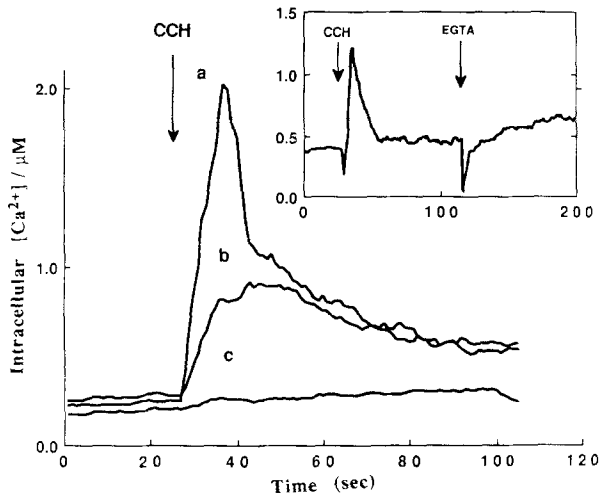

Fig. 2. Response of gastric gland intracellular calcium to carbachol; effect of the muscarinic antagonist 4-DAMP. Gastric glands, loaded with FURA2 as described in the text, were suspended at 20 mg/ml in monitoring solution containing (*a*) 0 nM, (*b*) 10 nM and (*c*) 1 μM 4-DAMP. At the indicated time, carbachol was added to a final concentration of 100 μM. Intracellular calcium was determined from the ratio of fluorescence at 340 and 380 nm. There appears to be a differential inhibition of the peak and elevated steady-state calcium levels. *Inset:* effect of $LaCl_3$ on the response of gastric gland $[Ca^{2+}]_i$ to 100 μM carbachol. Gastric gland calcium was monitored in FURA2-loaded glands suspended in solution A containing 20 μM La^{3+}. Following addition of 100 μM carbachol, 50 μM EGTA was added to chelate La^{3+}

As shown in Fig. 2 (trace *a*), addition of carbachol at 100 μM produced an initial rapid but transient peak rise of $[Ca^{2+}]_i$. The peak rise decayed to a lower steady-state level which was still above the basal concentration. Consistent with previous results (Muallem & Sachs, 1985) the elevated level eventually declined to resting levels over a period of 25–35 min, paralleling the transient time course of carbachol stimulated acid secretion. The results of several experiments are summarized in Table 1.

In this set of experiments, the basal $[Ca^{2+}]_i$ averaged 270 nM and the addition of carbachol resulted in an increase to 1600 nM at the peak of the transient, and to 670 nM at the steady-state elevated level. The pattern of $[Ca^{2+}]_i$ response to carbachol is similar to that seen in previous investigations (Negulescu et al., 1989), and suggests two phases of response involving an initial mobilization of intracellular calcium, accompanied or followed by an increase of membrane permeability to calcium.

This is supported by the experiment shown in the inset of Fig. 2. Here the intracellular calcium level is monitored in the presence of 20 μM La^{3+}, a blocker of calcium permeability. Addition of carbachol, under these conditions, results in a rapid peak response of $[Ca^{2+}]_i$ and a rapid return to basal level with no steady-state elevation. Subsequent addition of 50 μM EGTA, to complex the La^{3+} without removing external calcium, produced a steady-state elevation of $[Ca^{2+}]_i$, due to calcium influx. These results indicate that the two phases of the response are functionally independent.

The response of $[Ca^{2+}]_i$ to carbachol was found to be sensitive to muscarinic antagonists. As shown for 4-DAMP in Fig. 2, both the peak rise and the steady-state elevation are inhibited by the antagonists. When the two phases of the response are treated independently, both show a concentration-dependent inhibition by all antagonists tested. These results are presented in Fig. 3 and the estimated log IC_{50} values are given in Table 2. For both phases of the response, the general order of potency for the antagonists was found to be

4-DAMP = atropine ≫ pirenzepine ≫ AF-DX 116.

However, the peak response appears to be more sensitive to the antagonists, particularly to 4-DAMP and atropine, than is the steady-state elevation.

Acid Secretion

Acid secretory responses of gastric glands to carbachol and muscarinic antagonists were measured as aminopyrine accumulation or evolution of CO_2 from radiolabeled glucose. The results of these experiment are presented in Fig. 3 and Tables 1 and 2.

The aminopyrine accumulation ratio increased, on average, from 25 to 88 following the addition of 100 μM carbachol. The responses to carbachol were found to be concentration-dependent with an EC_{50} of 3.5 ± 0.3 μM ($n = 8$). It should be noted that these results were obtained in the presence of cimetidine and, while the response is somewhat lower than might be expected, it does reflect a direct effect of the cholinergic agonist on the parietal cells. The stimulation of acid secretion by carbachol was inhibited in a concentration-dependent manner by all of the muscarinic antagonists tested (Fig. 3). The IC_{50} values obtained from the experimental results were: 4-DAMP, 35 nM; atropine, 38 nM; pirenzepine, 13 μM; and, AF-DX 116, 110 μM (values derived from Table 2). The basal, i.e., without carbachol, aminopyrine accumulation and the increases in the accumulation ratio attendant on the stimulation of acid secretion by histamine or forskolin were unaffected by the muscarinic antagonists.

Stimulation of acid secretion by gastric glands is accompanied by an increase of oxidative metabolism as measured by oxygen consumption or glucose oxidation. The increase in metabolism is directly related to an increase in the activity of the parietal cell H,K-ATPase, since it is blocked by specific in-

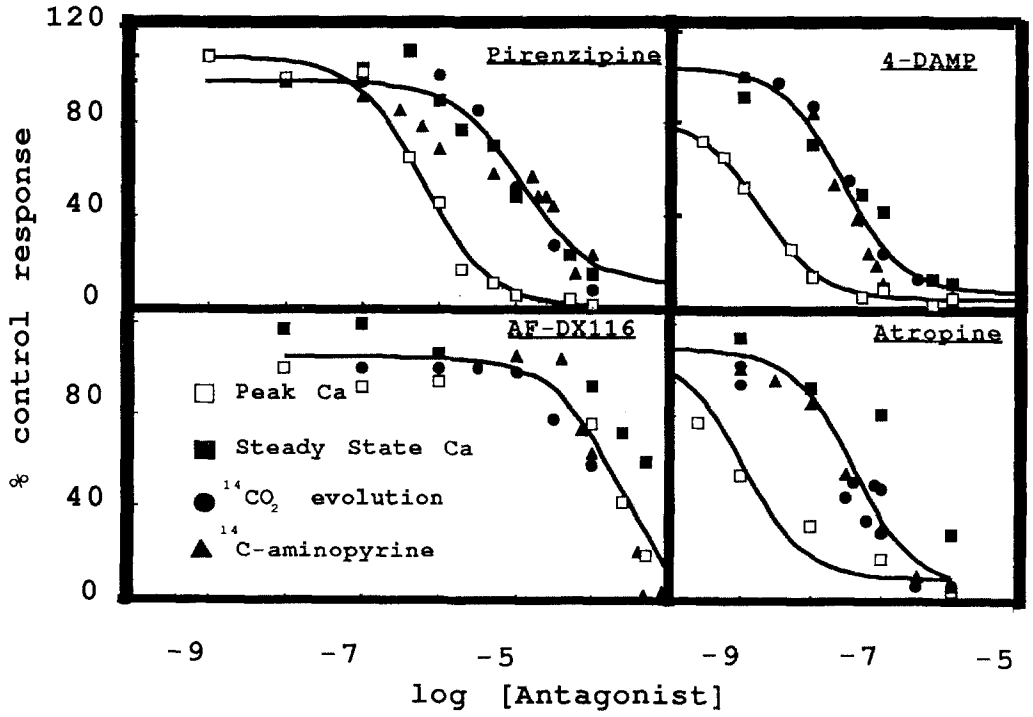

Fig. 3. Comparison of gastric gland responses to carbachol: effects of muscarinic antagonists. The responses of gastric gland steady-state calcium (■); aminopyrine accumulation (▲) and $^{14}CO_2$ evolution (●) to 100 μM carbachol in the presence of differing doses of muscarinic antagonists were expressed as percentages of control responses and fitted to a single dose response curve by nonlinear regression analysis. Peak calcium in response to carbachol (□) was analyzed separately, and curves were fitted to this data. The calculated log IC_{50} values are: pirenzepine, −4.93 + 0.14 (combined) and −6.20 + 0.08 (peak Ca); AF-DX116: −3.68 + 0.12 (combined) and −3.64 + 0.11 (peak Ca); 4-DAMP, −7.58 + 0.10 (combined) and −8.76 + 0.07 (peak Ca); atropine, −7.39 + 0.13 (combined) and −8.93 + 0.13 (peak Ca)

Table 2. Muscarinic antagonist efficacy against cellular responses of gastric glands stimulated by carbachol

Cellular response	log(IC_{50})			
	4-DAMP	Atropine	Pirenzipine	AF-DX 116
[^{14}C]-aminopyrine	−7.46 + 0.07	−7.42 + 0.05	−4.89 + 0.12	−3.96 + 0.27
$^{14}CO_2$ evolution	−7.45 + 0.13	−7.22 + 0.21	−4.61 + 0.13	−3.73 + 0.22
Steady-state elevated $[Ca^{2+}]_i$	−7.31 + 0.12	−6.61 + 0.51	−5.17 + 0.15	−3.31 + 0.28
Peak transient $[Ca^{2+}]_i$	−8.76 + 0.07	−8.93 + 0.13	−6.20 + 0.08	−3.64 + 0.11

Rabbit gastric glands were assayed for the response of several cellular properties to 100 μM carbachol in the presence of a range of muscarinic antagonist concentrations. Responses were expressed as a percentage of the control response, and dose response curves constructured for each antagonist and response. Efficacy of the antagonist is represented in the above table as the log IC_{50}, with standard error, calculated by nonlinear regression analysis.

hibitors of this enzyme, including omeprazole and SCH28080 (Fryklund et al., 1990). Exposure of the glands to carbachol resulted in an increase in the oxidation of ^{14}C-labeled glucose from a resting level of 102.9 to 172.5 nmol CO_2/hr · mg dry wt (Table 1). The increase in glucose oxidation was inhibited by the muscarinic antagonists in a concentration-dependent manner (Fig. 3).

The estimated IC_{50} values were: 4-DAMP, 35 nM; atropine, 60 nM; pirenzepine, 25 μM; and, AF-DX 116, 190 μM (values derived from Table 2). Evaluation of the data contained in Fig. 3 and Table 2 showed a close correlation between aminopyrine accumulation and CO_2 evolution with respect to the inhibition by muscarinic antagonists. This is to be expected since both parameters reflect the same bio-

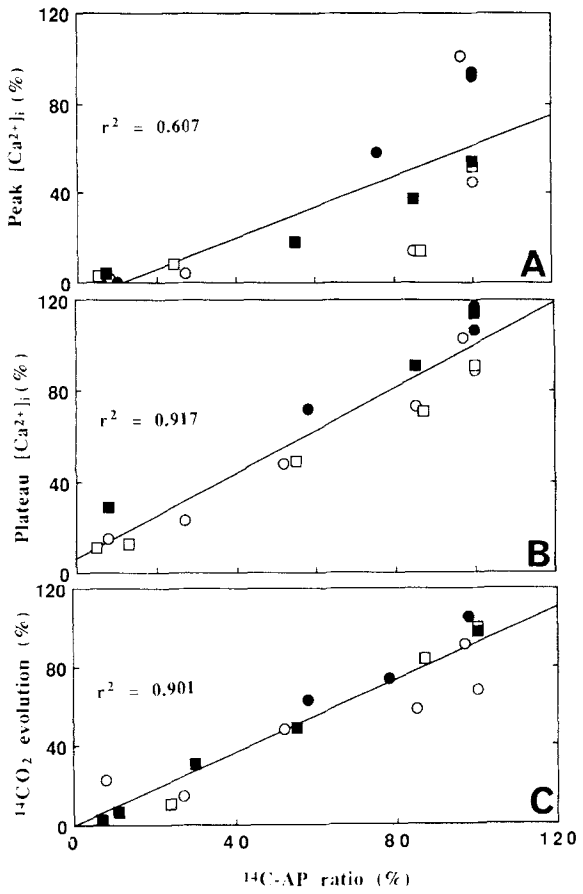

Fig. 4. Correlation between cellular responses of gastric glands to 100 μM carbachol. Percentage inhibition of peak and plateau calcium, $^{14}CO_2$ evolution and ^{14}C-aminopyrine accumulation were calculated. Pairwise combinations of aminopyrine accumulation and (*A*) peak $[Ca^{2+}]_i$, (*B*) plateau $[Ca^{2+}]_i$, (*C*) $^{14}CO_2$ evolution were subjected to regression analysis, and are displayed above. Inhibition was produced by the following antagonists at 10^{-10} M to 10^{-3} M (■) atropine, (○) pirenzepine, (●) AF-DX116 and (□) 4-DAMP

logical response to cholinergic stimulation. Also, there appears to be a good correlation between the acid secretory parameters and the steady-state elevation of $[Ca^{2+}]_i$.

However, the inhibition of the peak elevation of $[Ca^{2+}]_i$ correlates poorly with inhibition of acid secretion. In order to quantitate the relationships for the measured parameters, the data were subjected to regression analysis as shown in Fig. 4. Here the parameters are compared pairwise for inhibition by antagonists, in relation to aminopyrine accumulation. As anticipated, there is a strong correlation between aminopyrine accumulation and CO_2 production ($r^2 = 0.901$). The correlation between aminopyrine accumulation and steady-state elevation of $[Ca^{2+}]_i$ is equally strong ($r^2 = 0.917$), while little correlation ($r^2 = 0.607$) exists between aminopyrine accumulation and the initial peak rise of $[Ca^{2+}]_i$. The lack of correlation between acid secretion and the peak rise of $[Ca^{2+}]_i$ appears to reflect a greater sensitivity of this calcium response to all of the antagonists except for AFDX 116.

It was then possible using 10 nM DAMP to abolish the transient rise in $[Ca^{2+}]_i$, with no effect on either secretory parameter. Similar results were obtained using 10 nM TPA, an activator of protein kinase C, which presumably down regulates either release of Ca^{2+} from intracellular stores or the receptor or state of the receptor that responds to 4-DAMP.

Image Analysis of Intracellular Calcium

Gastric glands contain several cell types, including chief cells which display changes in $[Ca^{2+}]_i$ mediated by muscarinic cholinergic receptors (Chew & Brown, 1986). Therefore, the measurements of $[Ca^{2+}]_i$ using suspensions of glands may reflect a contribution from several cell types. To establish that at least in part the response is due to parietal cells image analysis was used, rather than cell separation. It has been our experience that CCh responsiveness of purified parietal cells is somewhat variable as compared to gastric glands. Digital image analysis has been used previously to isolate the response of specific gastric gland cells (Paradiso, Tsien & Machen, 1987), taking advantage of the anatomy of the gland.

A typical experiment applying image analysis to a gastric gland loaded with FURA2 is presented in Fig. 5. The ratioed image, coded in terms of calcium concentration, demonstrated that exposure of the glands to carbachol resulted in a rapid rise of $[Ca^{2+}]_i$. Individual cells are easily identified in these images. The large, bulbous cells at the periphery of the glands are readily distinguished from other cell types. These cells demonstrate the high densities of mitochondria characteristic of parietal cells when stained by the nitrotetrazolium blue-succinate method (Berglindh & Obrink, 1976), and are clearly the site of acid secretion, in that they accumulate the weak base acridine orange when gastric glands are treated with acid secretagogues (Rabon et al., 1983).

Although the response of individual cells varied considerably, significant changes of $[Ca^{2+}]_i$ were observed to occur in the identified parietal cells. Microscopic visualization also revealed that parietal cells loaded considerably higher levels of FURA2 than other cell types, showing that the parietal cell was the main source of the fluorescence signal derived from gastric glands in the cuvette experiments.

The image analysis technique was used to quantitate the response of individual parietal cells to addi-

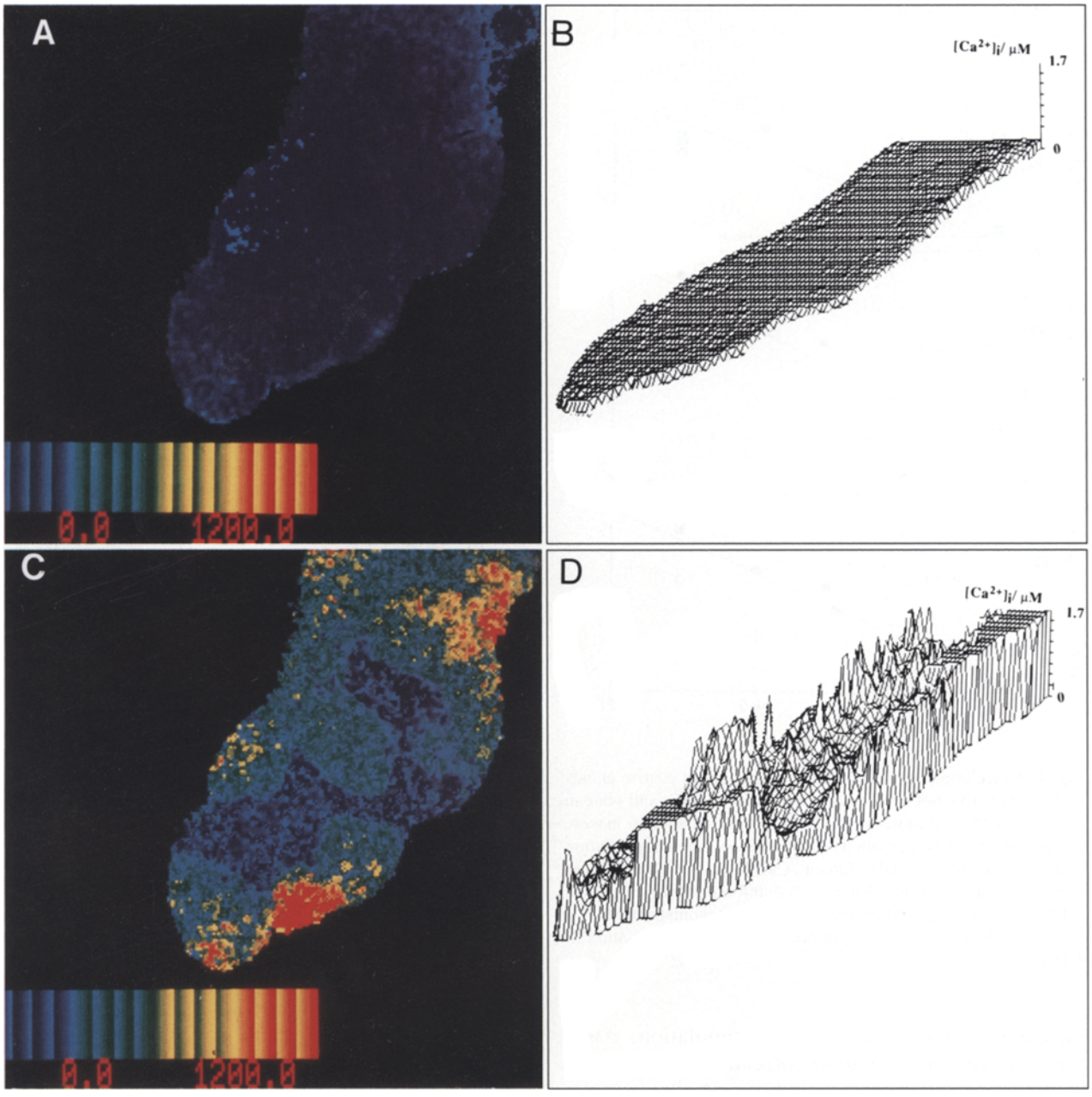

Fig. 5. Cellular resolution of $[Ca]_i$ levels by digital image analysis. Gastric glands loaded with FURA2 were observed through a Zeiss microscope in epifluorescence mode, with alternate illumination at 380 and 350 nm. Images were captured with an ISIT camera, and digitized in a JOYCE-LOEBL MAGISCAN image processing unit, under the control of TARDIS software. Perfusion of the gland with monitoring solution was followed by perfusion with a solution containing 100 μM carbachol. At the end of the experiment response of the dye to maximal and minimal Ca^{2+} was determined by sequential addition of 2 μM ionomycin and 20 mM EGTA. Spatial resolution of Ca^{2+} concentration was determined as described under Materials and Methods. (*A*) Spatial resolution of $[Ca]_i$ as measured in ratio mode in a gastric gland in resting state, displayed in pseudocolor (color scale adjacent to the picture). (*B*) Calcium concentration over gastric gland shown in *A*; displayed as a perspective plot. (*C*) Distribution of calcium in pseudocolor following 17 sec exposure to 100 μM carbachol. (*D*) Perspective plot of Ca concentration in gastric gland following exposure to 100 μM carbachol

tion of carbachol. Eleven individual parietal cells, observed in two separate experiments, were analyzed and the time course of the response to carbachol is presented in Fig. 6*A*. In these experiments, the response of individual parietal cells is seen to be consistent with the responses obtained for glands in suspension.

Accordingly, there is a rapid, transient rise of

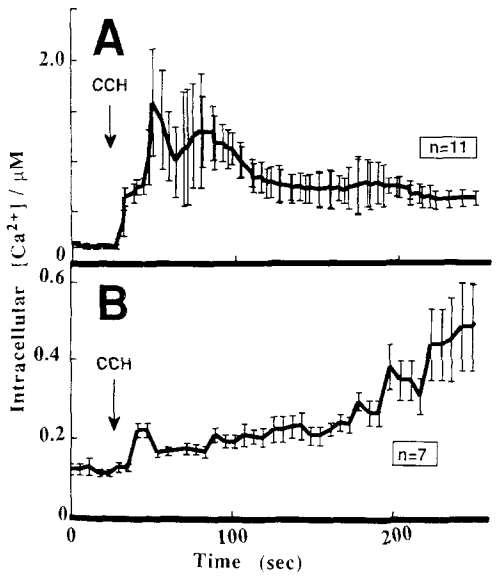

Fig. 6. Analysis of individual parietal cell responses to carbachol. Gastric glands, loaded with FURA2, were subjected to digital image analysis as previously described. From the sequences, resolved in terms of intracellular calcium concentration, the calcium concentrations of identified parietal cells were determined over the course of the experiment. Perfusions were performed using monitoring solution (upper panel) or monitoring solution plus 10 nM 4-DAMP (lower panel; note differences in scale). The time courses show the response to 100 μM carbachol and are displayed as mean and 1 SD for *n* cells in the two experiments

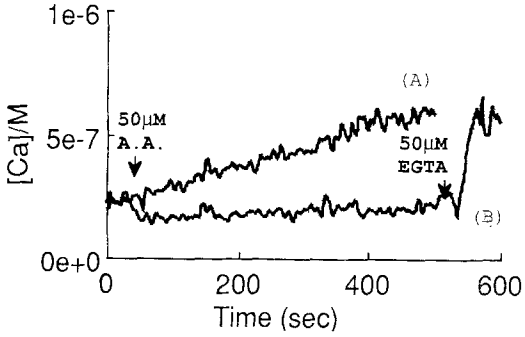

Fig. 7. Effect of arachidonic acid on gastric gland intracellular calcium. Gastric glands, loaded with FURA2 as described in the text, were suspended at 20 mg/ml in monitoring solution (*A*), or monitoring solution plus 20 μM $LaCl_3$ (*B*). At the indicated time arachidonic acid was added to a final concentration of 50 μM. 50 μM EGTA was added to the glands in trace (*B*) in order to reverse the effect of lanthanum

$[Ca^{2+}]_i$ which declines to a steady-state elevated level. These results indicate that the parietal cells are responsible, at least in part, for the biphasic response of $[Ca^{2+}]_i$ to carbachol and that the apparent lack of correlation between the initial rise in calcium and acid secretion is not due to cellular heterogeneity.

One test of the relationship between acid secretion and the two phases of $[Ca^{2+}]_i$ response by parietal cells is suggested by the differential sensitivity of the two phases to the antagonist, 4-DAMP in the cuvette experiments. With IC_{50} values for 4-DAMP of 1.7 nM *versus* the initial rise, and 49 nM *versus* the steady-state elevation, it may be calculated that 10 nM 4-DAMP would inhibit 82% of the peak transient response, while inhibition of the steady state would be only about 15%.

To validate this calculation, individual parietal cells were monitored with the image analysis system. The glands were exposed to carbachol (10^{-4} M) in the presence of 10 nM 4-DAMP, and the $[Ca^{2+}]_i$ responses were determined. The results obtained for seven individual parietal cells are presented in Fig. 6*B*. The presence of 4-DAMP at 10 nM produced a complete inhibition of the initial peak response to carbachol in the parietal cells, but did not prevent the $[Ca^{2+}]_i$ from rising slowly to a new steady-state level.

It should be noted (Fig. 3) that this concentration of 4-DAMP produces little, if any, inhibition of acid secretion. In addition, the presence of 10 nM 4-DAMP neither inhibits or accentuates the transient time course of the acid secretory response to carbachol. The signals obtained in the cuvette, therefore, correlate with the single cell analyses of parietal cell fluorescence.

Effect of Arachidonic Acid and Ionomycin

It has been suggested that arachidonic acid liberated from membrane phospholipids by phospholipase action may have a second messenger role (Conklin et al., 1988). Figure 7 demonstrates that addition of 50 μM arachidonic acid to isolated gastric glands induced an elevation of intracellular calcium, inhibitable by 20 μM La^{3+}. The magnitude of response and the EGTA reversible sensitivity to La^{3+} were similar to the elevated state induced by carbachol. However, when the secretory response of the glands was measured with either aminopyrine accumulation or with CO_2 production, no effect was observed.

The titration of $[Ca]_i$ with ionomycin also produced a steady-state elevation of Ca levels. How-

ever, although it was not possible to exclude artifacts on aminopyrine accumulation in the presence of this Ca/2H exchange ionophore, it could be shown that CO_2 production was not elevated by this maneuver. Hence both means of elevation of $[Ca]_i$ were ineffective in mimicking the acid secretory effects of CCh.

Accordingly, it is possible to eliminate the transient (i.e., activation of PLC and production of IP_3 and diacyl glycerol without affecting acid secretion. From earlier data as discussed above, a change in steady-state $[Ca]_i$ is, however, necessary for, but therefore insufficient for, acid secretion.

Binding Studies

Binding of ^{3}H-NMS to parietal cells gave results consistent with a single class of sites with a K_{dapp} of 0.23 ± 0.03 nM (mean ± SEM; n= 5). Displacement of NMS by 4-DAMP fitted a single site model as shown in Fig. 8. The slope of the pseudo-Hill plot was 0.85 ± 0.03 (mean ± SEM; n= 4) and the K_{dapp} was 1.7 nM. In contrast, the displacement of NMS by carbachol showed the presence of two classes of sites. The pseudo-Hill plot had a slope of 0.70 ± 0.01 (mean ± SEM; n =3) and the calculated K_{dapp} were 1.3 μM for the higher affinity site and 71 μM for the low affinity site. Hence the selective action of DAMP on function and Ca signalling can be explained by two CCh affinities in the preparation. The low affinity site is displaced by 4-DAMP with high affinity, whereas the high affinity site is displaced by 4-DAMP with low affinity, since 4-DAMP is a competitive inhibitor at muscarinic sites. The high affinity CCh site is therefore coupled to acid secretion and hence to elevation of steady-state $[Ca]_i$.

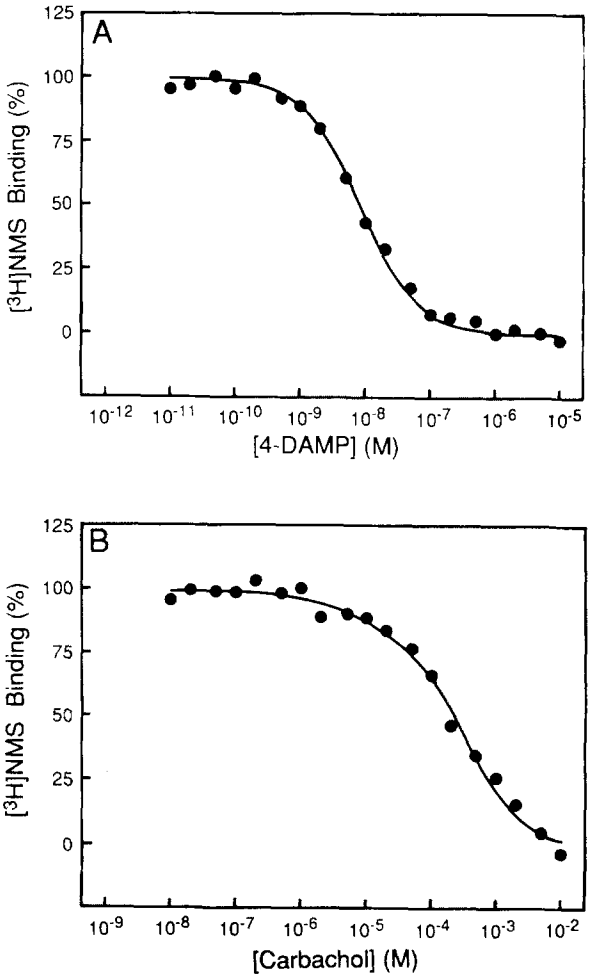

Fig. 8. Displacement of ^{3}H-NMS binding to purified parietal cells by 4-DAMP and carbachol. The methods are detailed in the text. The specific binding of NMS in the absence of ligands was set at 100%. The IC_{50} values calculated as described were for 4-DAMP 8.6 nM, and for carbachol 6.6 μM (16%) and 350 μM (84%) A. displacement by 4-DAMP B. Displacement by carbachol

Discussion

Cholinergic stimulation of gastric acid secretion has long been recognized, but the underlying specific receptor and second messenger pathways are ill defined. In vivo, acetylcholine may affect secretion by neural or hormonal pathways, while in vitro stimulation of the parietal cell could be a direct or an indirect action of cholinergic agonists, since histamine release is one of the actions of cholinergic stimulation of rabbit gastric glands.

In the present study, stimulation of acid secretion by carbachol was measured in the presence of cimetidine, eliminating the indirect pathway. The finding that the acid secretory response was blocked by selective antagonists confirms previous suggestions that the parietal cell possesses muscarinic receptors (Culp et al., 1983), and that these receptors mediate acid secretion directly (Soll 1978; Berglindh, 1977*b*).

The data presented confirm the previous reports that cholinergic stimulation in a number of glandular cell types is associated with a rise in $[Ca^{2+}]_i$ (Muallem & Sachs, 1985; Chew & Brown 1986; Negulescu et al., 1989; Brown & Chew 1989; Merrit & Rink, 1987) and provide direct evidence that the changes in $[Ca^{2+}]_i$ described above reflect responses of the parietal cell.

The response of $[Ca^{2+}]_i$ to carbachol was found to be biphasic, consisting of an initial transient phase and a steady-state elevation. This is characteristic of Ca signalling in most nonexcitable cells.

Both phases were shown to occur within individual parietal cells using image analysis, demonstrating that the biphasic time course is not due to cellular heterogeneity, but that it is a parietal cell response. The geometry of the gland allows visualization of the parietal cell cytoplasm without contamination from the chief cells and, in any case, the chief cell loaded significantly less well with fura 2 in this preparation.

Further evidence for the muscarinic response being studied here being mainly a property of parietal cells was obtained by binding studies in purified parietal cells. Two sites were obtained for CCH displacement of NMS binding, which would predict differential displacement of CCH by 4-DAMP and therefore be consistent with the separation of the CCh-stimulated $[Ca]_i$ changes by 4-DAMP. The higher CCh affinities for binding are the same as for stimulation of acid secretion, again consistent with $[Ca]_i$ and functional effects.

The two phases of the calcium response were easily separated. Thus, low concentrations of La^{3+} block the steady-state rise but not the initial transient. Conversely, low concentrations of 4-DAMP block the initial rise while allowing the slower steady-state increase. The same result is obtained with TPA at 10nM concentration. The initial transient rise of $[Ca^{2+}]_i$ also was found to be more sensitive to atropine and pirenzepine than was the steady-state elevation. Based on these observations, it seems the two phases of the calcium response to carbachol are independently regulated. They are mediated either by different subtypes of muscarinic receptors or by the same subtype that is differentially coupled.

Transient or biphasic responses of $[Ca^{2+}]_i$ to stimulation have been found in a variety of tissues. In general, the initial response is believed to be due to a release of calcium from an intracellular storage site (Rana & Hokin, 1990), while the steady-state elevation is thought to result from an increase in the plasma membrane permeability to calcium (Petersen & Muruyama, 1983). This seems also to be the case for the parietal cell, since La^{2+}, which prevents membrane permeation of Ca, selectively blocks the steady-state rise of $[Ca^{2+}]_i$. The observation that the calcium which contributes to the two phases of the response is derived from different sources, suggests that the intracellular mechanisms which couple muscarinic receptor activity to changes in calcium also are different.

There is substantial evidence that the release of calcium from intracellular stores, i.e., the initial phase, is mediated by phospholipase C and the generation of inositol trisphosphate (Rana & Hokin, 1990). This is supported in the case of the parietal cell by the observation that cholinergic stimulation is associated with an increase in the production of inositol trisphosphate (Chew & Brown, 1986). The DAG produced presumably is able to active protein kinase C. It is perhaps not surprising that the C kinase activator, TPA, appears to be able to exert feedback inhibition of this pathway without affecting Ca entry or acid secretion.

In the presence of low concentrations of 4-DAMP (or TPA), carbachol was found to increase the membrane permeability to calcium without producing a release of calcium from an intracellular pool, and thus presumably without activating phospholipase C. Therefore, it may be suggested that the steady-state elevation of $[Ca^{2+}]_i$ is not mediated by phospholipase C, nor by its products, inositol phosphates and diacylglycerol and can occur without changes in these intermediates. An as yet unidentified coupling mechanism must be present, usually called a receptor-operated Ca channel (ROC). This hypothesis is shown in the model presented in Fig. 9.

A second major objective of the present studies was to investigate the quantitative relationship between acid secretion and $[Ca^{2+}]_i$ as revealed by selective antagonism of cholinergic responses. Using four muscarinic antagonists, a strong correlation was found between inhibition of acid secretion and inhibition of the steady-state elevation of $[Ca^{2+}]_i$. Since pirenzepine blocked function with lower affinity than 4-DAMP and AFDX 116 with even lower affinity, it is likely that 4-DAMP is detecting an M3 receptor subtype coupled to secretion and Ca changes.

There appeared to be no correlation between acid formation and the initial rise of $[Ca^{2+}]_i$. Thus, it is concluded that acid secretion is mediated by the sustained influx of calcium across the plasma membrane and not by the release of calcium from an intracellular pool. This conclusion is supported by the following observations. (i) La^{3+}, which selectively inhibits the steady-state increase of calcium, blocks acid secretory responses (Muallem & Sachs, 1985). (ii) In the absence of external calcium, CCh-stimulated acid secretion in isolated gastric glands is reduced (Chew, 1985) or abolished (Berglindh et al., 1980). (iii) Concentrations of 4-DAMP which selectively inhibit the transient phase do not inhibit acid secretion when the steady-state elevation of calcium is unaffected. (iv) Reduction of intracellular calcium in parietal cells loaded with the chelating agent 1,2-bis(2-aminophenoxy)ethane-N,N,N',N'-tetraacetic acid (BAPTA) abolished the stimulation of acid secretion by CCh (Brown & Chew, 1989;

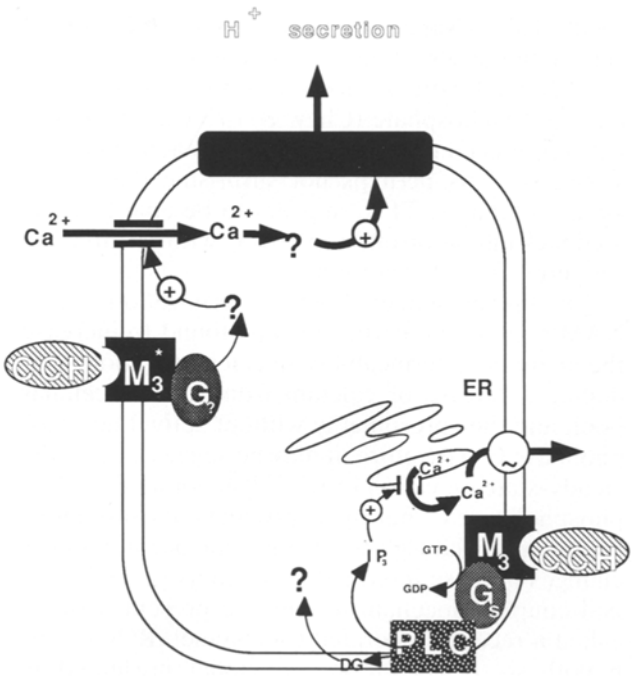

Fig. 9. Model of mechanisms modulating intracellular calcium in the rabbit parietal cell. The parietal cell possesses two populations of receptors, putatively of the M3 subtype, of differing affinity for muscarinic agonists. The high affinity receptor (designated M_3^*) is responsible for modulating the plasma membrane permeability to Ca^{2+} and hence produces a sustained elevation in the level of $[Ca^{2+}]_i$ (from 0.27 to 0.67 μM). This is highly correlated with the observed stimulation of acid secretion and with the documented dependence of muscarinic stimulation on external calcium indicates a role for elevated $[Ca^{2+}]_i$ in the stimulation of acid secretion. The low affinity state of the receptor is responsible for the rapid, transient increase in $[Ca^{2+}]_i$ due to mobilization of intracellular stores. This is due to coupling of the receptor-ligand complex to phospholipase C (PLC) by a G-protein phospholipase C acts upon phosphatidylinositol 4,5-bisphosphate in the membrane, releasing inositol 1,4,5-trisphosphate (IP_3), and di-acyl glycerol (DAG). It is not known if DAG has any further role in cell signalling other than inhibition of Ca release due to activation of protein kinase C. IP_3 interacts with a receptor on the endoplasmic reticulum, producing rapid release of Ca^{2+}, which is subsequently pumped out of the cell by the action of the Ca^{2+}-activated ATPase. The parietal cell demonstrates essentially normal acid secretory states when antagonist concentrations are applied which selectively abolish the peak, but not elevated steady-state calcium response. The rapid transient therefore has no apparent role in acid secretion

Negulescu et al., 1989). (v) Two binding affinities on purified parietal cells were detected for CCh displacement of ^{3}H-NMS, and the displacement affinity of 4-DAMP was higher than that of the other selective antagonists.

In a recent paper, examining the effects of muscarinic agonists on parietal cell calcium and acid secretion, evidence was presented which was interpreted as a correlation between the magnitude of the initial peak response of $[Ca^{2+}]_i$ and secretion (Negulescu et al., 1989). Since the present studies were performed in the presence of the histamine antagonist, cimetidine, it may be that the above data were related more to histamine release that to direct action of CCh on the parietal cell, since no H2 antagonist was present in their preparation. As noted above, the acid secretory response of isolated gastric glands to carbachol is less than that obtained with histamine, histamine interacts synergistically with carbachol, and gastric glands contain cell types which are able to release histamine as a local effector. Thus, in the absence of a histamine antagonist, higher concentrations of carbachol could cause a release of histamine by binding at a low affinity site on the ECL cell and thereby shift the concentration-response relationship for cholinergic stimulation of acid secretion to the right as histamine comes into play. In support of this possibility is the finding of a lower EC_{50} value for carbachol stimulation of aminopyrine accumulation in this study (3.5 μM) as compared to the previous report of 18 μM (Negulescu et al., 1989).

In addition to examining quantitative relationships, the use of selective antagonists in the present study allowed further identification of the subtypes of muscarinic receptors which mediate parietal cell responses. In recent years, the muscarinic receptors have been divided into a number of subtypes, initially by the use of selective antagonists, and subsequently by molecular cloning of the individual subtypes. Antagonist studies have resulted in a variety of classification schemes (Mitchelson, 1988; Hulme et al., 1990), but the identification of subtypes at the molecular level is simplifying the classification.

To date, five muscarinic receptor subtypes have been isolated and sequenced (Buckley et al., 1989; Liao et al., 1989). All of the subtypes are coupled to regulatory G-proteins and show structural and functional similarities (Liao et al., 1989). In the present study, the muscarinic antagonists inhibited acid secretion and $[Ca^{2+}]_i$ responses with the order of potency: 4-DAMP $\gg$ pirenzepine $>$ AF-DX 116. This pattern of inhibition is characteristic of the M3 (glandular) receptor subtype and is consistent with the pattern of antagonist potency against a cloned M3 type receptor expressed in transfected cells (Pinkas-Kramarski et al., 1988; Buckley et al., 1989). Additionally, recent antagonist profile studies have indicated that cholinergic stimulation of isolated rat parietal cell acid secretion is mediated by an M3 type muscarinic receptor (Pfieffer et al., 1990), consistent with our identification of an M3 receptor in rabbit parietal cells. In addition to differences in antagonist affinity, the muscarinic receptor subtypes display

differences in the mechanisms which mediate the responses. The M2 and M4 subtypes appear to down regulate adenylate cyclase, whereas the M1, M3 and M5 subtypes appear to regulate phospholipid metabolism and intracellular calcium (Conklin et al., 1988; Liao et al., 1989). Since the cholinergic stimulation of the parietal cell is associated with changes in intracellular calcium rather than cyclic AMP, the type of receptor coupling also would favor designation of the parietal cell muscarinic receptor as an M3 subtype.

Although both phases of the $[Ca^{2+}]_i$ response displayed the same potency sequence for antagonists, there are some significant differences in antagonist affinity. Specifically, the peak response is more sensitive to 4-DAMP, atropine, and pirenzepine but has a similar affinity for AF-DX 116 as compared to the steady-state response. The similar potency sequence indicates that both phases are mediated by M3 subtype receptors. However, the differences in antagonist affinities, and the probable difference in coupling mechanisms indicates that the receptors mediating the two phases are not identical. A partial explanation for the differences in antagonist affinities may lie in the observation that the initial transient calcium response displays a lower affinity (higher EC_{50}) for carbachol than does the steady-state elevation (Negulescu et al., 1989). Since the IC_{50} for a competitive antagonist, as measured in the present studies, is directly related to the agonist affinity (Cheng & Prusoff, 1973), the lower IC_{50} values for 4-DAMP inhibition of the initial calcium response could be attributed to the lower agonist affinity for this phase. Thus, it may be suggested that the initial transient phase of the calcium response is mediated by an M3 receptor with low agonist affinity, while the steady-state elevation is mediated by an M3 receptor with high affinity for agonists. This suggestion is consistent with the different mediation mechanisms displayed by the two phases, since it is known that the receptor affinity for agonists can be modified by the coupling G-proteins (Florio & Sternweiss, 1985). The two affinities also correspond to the two binding displacement affinities displayed by CCh in isolated parietal cells.

In support of this hypothesis, Pinkas-Kramarski et al. (1989) expressed M3 type receptors in a cell line lacking endogenous receptors. In displacement binding assays these receptors demonstrated a high and low affinity population when probed with pirenzepine and 4-DAMP, but only a single, low affinity state was observed with respect to AF-DX 116. Thus AF-DX 116 does not discriminate between the two affinity states distinguished by the other antagonists. Furthermore, the high affinity state was converted to the low affinity state by the addition of nonhydrolyzable GTP analogues, indicating that G-proteins may determine the high and low affinity states.

Cholinergic stimulation of the parietal cell appears to involve a dual signal consisting of a high affinity M3 receptor which regulates calcium permeability of the plasma membrane by an unknown mechanism and a low affinity M3 receptor which activates phospholipase C and hence mobilizes calcium from an intracellular pool. The former signal is linked to activation of the acid secretory mechanism, while the latter serves an as yet unknown function.

The elevation of intracellular calcium does not appear sufficient to promote the acid secretory effect, although it is a necessary component of the process. Elevation of intracellular calcium by ionomycin appears to result in the phosphorylation of a protein involved in carbachol induced acid secretion (Brown & Chew, 1989). However, elevation of calcium to agonist-induced levels by ionomycin or by exposure to various levels of arachidonic acid (1–100 μM) did not stimulate gastric gland acid secretory activity when monitored by aminopyrine accumulation or CO_2 evolution.

Hence the parietal cell shows a pattern of $[Ca]_i$ responses to activation of an M_3 receptor that suggest coupling of secretion to steady-state changes of $[Ca]_i$. However, although $[Ca]_i$ changes are a necessary accompaniment of change in transport, they may be insufficient on their own to activate secretion.

M.K. was supported by a fellowship from Marion Laboratories, Kansas City, MO.

References

Berglindh, T. 1977*a*. Potentiation by carbachol and aminophylline of histamine and db-cAMP induced parietal cell activity in isolated gastric glands. *Acta Physiol. Scand.* **99:**75–84

Berglindh, T. 1977*b*. Effects of common inhibitors of gastric acid secretion on secretagogue induced respiration and aminopyrine accumulation in isolated gastric glands. *Biochim. Biophys. Acta* **464:**217–233

Berglindh, T., Helander, H.F., Obrink, K.J. 1976. Effects of secretagogues on oxygen consumption, aminopyrine accumulation and morphology in isolated gastric glands. *Acta Physiol. Scand.* **97:**401–414

Berglindh, T., Obrink, K.J. 1976. A method for preparing isolated gastric glands from rabbit gastric mucosa. *Acta Physiol. Scand.* **96:**150–159

Berglindh, T., Sachs, G., Takeguchi, N. 1980. Ca^{2+} dependent secretagogue stimulation in isolated gastric glands. *Am. J. Physiol.* **239:**G90–G94

Bergqvist, E., Obrink, K.J. 1979. Gastrin-histamine as a normal sequence in gastric acid stimulation in the rabbit. *Uppsala J. Med. Sci.* **84:**145–154

Brown, M.R., Chew, C.S. 1989. Carbachol induced protein phos-

phorylation in parietal cells: Regulation by $[Ca_{2+}]_i$. *Am. J. Physiol.* **257:**G99–G110

Buckley, N.J., Bonner, T.I., Buckley, T.I., Brann, M.R. 1989. Antagonist binding properties of five cloned muscarinic receptors expressed in CHO-K1 cells. *Mol. Pharmacol.* **35:**469–476

Cheng, Y., Prusoff, W.H. 1973. Relationship between the inhibition constant (KI) and the concentration of an inhibitor that causes a fifty percent inhibition (IC_{50}) of an enzymatic reaction. *Biochem. Pharmacol.* **22:**3099–3108

Chew, C.S. 1985. Differential effects of extracellular calcium removal and non-specific effects of Ca^{2+} antagonists on acid secretory activity in isolated gastric glands. *Biochim. Biophys. Acta* **846:**370–378

Chew, C.S., Brown, M.R. 1986. Release of intracellular Ca^{2+} and elevation of inositol triphosphate by secretagogues in parietal and chief cells isolated from rabbit gastric mucosa. *Biochim. Biophys.Acta* **888:**116–125

Chew, C.S., Hersey, S.J., Sachs, G., Berglindh, T. 1980. Histamine responsiveness of isolated gastric glands. *Am. J. Physiol.* **238:**G312–G320.

Conklin, B.R., Brann, M.R., Buckley, N.J., Ma, A.L., Bonner, T.I., Axelrod, J. 1988. Stimulation of arachidonic acid release and inhibition of mitogenesis by cloned genes for muscarinic receptor subtypes stably expressed in A9L cells. *Proc. Natl. Acad. Sci. USA* **85:**8698–8702

Culp, P.J., Wolosin, J.M., Soll, A.H., Forte, J.G 1983. Muscarinic receptors and guanylate cyclase in mammalian gastric cells. *Am. J. Physiol.* **245:**G641–G646

Florio, V.A., Sternweiss, P.C. 1985. Reconstitution of resolved muscarinic cholinergic receptors with purified GTP binding proteins. *J. Biol. Chem.* **260:**3477–3483

Fryklund, J., Gedda, K., Scott, D., Sachs, G., Wallmark, B. 1990. Coupling of H^+K^+-ATPase activity and glucose oxidation in gastric glands. *Am. J. Physiol.* **258:**G719–G727

Grykiewicz, G., Poenie, M., Tsien, R.Y. 1985. A new generation of Ca^{2+} indicators with greatly improved fluorescence properties. *J. Biol. Chem.* **260:**3440–3450

Hersey, S.J. 1977. Metabolic changes associated with gastric stimulation. *Gastroenterology* **73:**914–919

Hersey, S.J., Chew, C.S., Campbell, L., Hopkins, E. 1981. Mechanism of action of SCN in isolated gastric glands. *Am. J. Physiol.* **240:**G232–G238

Hirschowitz, B.I., Molina, E. 1983. Effects of four H2 histamine antagonists on bethanechol stimulated acid and pepsin secretion in the dog. *J. Pharmacol. Exp. Ther.* **224:**341–345

Hulme, E.C., Birdsall, N.J.M., Buckley, N.J. 1990. Muscarinic receptor subtypes. *Ann. Rev. Pharmacol. Toxicol.* **30:**633–673

Kajimura, M., Haga, T., Ichiyama, A., Kaneko, E., Honda, N. 1990. Carbachol induced potentiation and inhibition of acid secretion by guinea pig gastric gland. *Eur. J. Pharmacol.* **178:**59–69

Liao, C.F., Themmen, A.P.N., Joho, R., Barberis, C., Birnbaumer, M., Birnbaumer, L. 1989. Molecular cloning and expression of a fifth muscarinic acetylcholine receptor. *J. Biol. Chem.* **265:**7328–7337

Merrit, J.E., Rink, T.J. 1987. Regulation of cytosolic free calcium in fura-2 loaded rat parotid acinar cells. *J. Biol. Chem.* **262:**17362-17369

Mitchelson, F. 1988. Muscarinic receptor differentiation. *Pharmacol. Ther.* **37:**357–423

Muallem, S., Blissard, D., Cragoe, E.J., Sachs, G. 1988. Activation of the Na/H and Cl/HCO_3 exchange by stimulation of acid secretion in the parietal cells. *J. Biol. Chem.* **263:**14703–14711

Muallem, S., Burnham, C., Blissard, D., Berglindh, T., Sachs, G. 1985. Electrolyte transport across the basal lateral membrane of the parietal cell. *J. Biol. Chem.* **260:**6641–6653

Muallem, S., Sachs, G. 1985. Ca^{2+} metabolism during cholinergic stimulation of acid secretion. *Am. J. Physiol.* **248:**G216–G228

Negulescu, P.A., Reenstra, W.W., Machen, T.E. 1989. Intracellular Ca requirements for stimulus-secretion coupling in parietal cell. *Am. J. Physiol.* **256:**C241–C251

Paradiso, A.M., Tsien, R.Y., Machen T.E. 1987. Digital image processing of intracellular pH in gastric oxyntic and chief cells. *Nature* **325:**447–450

Petersen, O.H., Muruyama, Y. 1983. What is the mechanism of the calcium influx to pancreatic acinar cells evoked by secretagogues? *Pfluegers Arch.* **396:**82–84

Pfieffer, A., Rochlitz, H., Noelke, B., Tacke, R., Moser, U., Mutschler, E., Lambrecht, G. 1990. Muscarinic receptors mediating acid secretion in isolated rat gastric parietal cells are of M3 type. *Gastroenterology* **98:**218–222

Pinkas-Kramarski, R., Stein, R., Zimmer, Y., Sokolovsky, M. 1988. Cloned rat M3 muscarinic receptors mediate phosphoinositide hydrolysis, but not adenylate cyclase inhibition. *FEBS Lett.* **239:**174–178

Rabon, E., Cuppoletti, J., Malinowska, D., Smolka, A., Helander, H.F., Mendlein, J., Sachs, G. 1983. Proton secretion by the gastric parietal cell. *J. Exp. Biol.***106:**119–133

Rana, R.S., Hokin, L.E. 1990. Role of phosphoinositides in transmembrane signalling. *Physiol. Rev.* **70:**115–164

Schubert, M.L., Bitar, K.N., Makhlouf, G.M. 1982. Regulation of gastrin and somatostatin secretion by cholinergic and noncholinergic intramural neurons. *Am. J. Physiol.* **243:** G442–G447

Soll, A.H. 1978. The interaction of histamine with gastrin and carbamylcholine in oxygen uptake by isolated mammalian parietal cells. *J. Clin. Invest.* **61:**381–389

Sutliff, V.E., Rattan, S., Gardner, J.D., Jensen, R.T. 1989. Characterisation of cholinergic receptors mediating pepsinogen secretion from chief cells. *Am. J. Physiol.* **257:**G226–G234

Received 15 June 1990; revised 23 January 1991